Journal of Alloys and Compounds 508 (2010) 238–244

Contents lists available at ScienceDirect

Journal of Alloys and Compounds

journal homepage: www.elsevier.com/locate/jallcom

Tricritical point and critical exponents of $La_{0.7}Ca_{0.3-x}Sr_xMnO_3$ ($x = 0$, 0.05, 0.1, 0.2, 0.25) single crystals

M.H. Phan[a,*], V. Franco[a,b], N.S. Bingham[a], H. Srikanth[a], N.H. Hur[c], S.C. Yu[d]

[a] Department of Physics, University of South Florida, Tampa, FL 33620, USA
[b] Dpto. Física de la Materia Condensada, ICMSE-CSIC, Universidad de Sevilla, P.O. Box 1065, Sevilla 41080, Spain
[c] Department of Chemistry, Sogang University, Seoul 121-742, Republic of Korea
[d] Department of Physics, Chungbuk National University, Cheongju 361-763, South Korea

ARTICLE INFO

Article history:
Received 29 July 2010
Accepted 30 July 2010
Available online 11 August 2010

PACS:
75.30.Sg

Keywords:
Doped manganites
Magnetic transition
Critical phenomena
Magnetoresistance

ABSTRACT

The nature of ferromagnetic phase transition and its critical properties in $La_{0.7}Ca_{0.3-x}Sr_xMnO_3$ ($x = 0$, 0.05, 0.1, 0.2 and 0.25) single crystals have been studied systematically. Based on magnetic measurements and critical behavior analysis using Banerjee criterion and Kouvel–Fisher method, we demonstrate the existence of a tri-critical point, with critical exponents ($\beta = 0.26 \pm 0.01$, $\gamma = 1.06 \pm 0.02$) at $x \sim 0.1$, that separates "discontinuous" first-order magnetic transition (FOMT) for $x < 0.1$ compositions from "continuous" second-order magnetic transition (SOMT) for $x > 0.1$ compositions. Above the tricritical point, the system (e.g. $x = 0.2$) shows a SOMT with the critical exponents ($\beta = 0.36 \pm 0.01$, $\gamma = 1.22 \pm 0.01$) belonging to the Heisenberg universality class ($\beta = 0.365 \pm 0.003$, $\gamma = 1.336 \pm 0.004$). This suggests that the magnetic interaction in these manganites is of short-range type. Our systematic studies show that chemical (internal) pressure induced by substituting larger Sr ions for smaller Ca ions, cooperative Jahn–Teller distortions, antiferromagnetic coupling, and formation of ferromagnetic clusters all have significant impact on the nature of the ferromagnetic phase transition, the conduction mechanism and colossal magnetoresistance (CMR) in the doped manganites.

1. Introduction

The discovery of colossal magnetoresistance (CMR) in doped manganites with the general formula $R_{1-x}M_xMnO_3$ (R = La, Pr, Nd, Sm, and M = Sr, Ca, Ba, and Pb) has stimulated intense research into their physical properties [1]. The relationship between the ferromagnetism and conductivity (e.g. the relationship between the metal–insulator (MI) transition and the paramagnetic–ferromagnetic (PM–FM) transition) in several CMR materials has continued to generate interest and reveal new insights, primarily due to the complexity of the systems [2–7]. It has been experimentally shown that while the parent compound $RMnO_3$ is an insulating antiferromagnet, substitution of the trivalent R^{3+} ion by a divalent M^{2+} ion leads to coexistence of Mn^{3+} and Mn^{4+} ions and, at sufficiently high doping levels (x), the material becomes a conductive ferromagnet [1]. The A-site (A = R, M) doping has been shown to control an effective one-electron bandwidth (W) which primarily governs the magnetic and magnetotransport properties of the materials [1–7]. The metallic ferromagnetic state in doped manganites was widely interpreted using the double-exchange (DE) mechanism [8,9]. According to this model, the transfer of an itinerant e_g electron between the neighboring Mn sites (local t_{2g} spins) through the O^{2-} ion results in a ferromagnetic interaction due to the on-site Hund's rule coupling. The strength of the DE interaction is evaluated by the transfer integral, $t_{eff} = t_0 \cos(\Theta/2)$ (Θ is a relative angle between the local spins). As a magnetic field is applied to the material, it will force the local t_{2g} spins to align thus reducing spin scattering (i.e. resistivity decreases) and enhancing the ferromagnetic phase. The DE theory has been shown to describe quite well the properties of the metallic ferromagnetic state in doped manganites with relatively large W, such as $La_{0.7}Sr_{0.3}MnO_3$ [10]. However, it alone cannot explain the features of the MI transition and CMR observed in manganites with narrow W such as $La_{0.7}Ca_{0.3}MnO_3$ [3], where other effects such as collective Jahn–Teller (JT) distortions and antiferromagnetic (AFM) interactions coexist and strongly compete with the ferromagnetic phase. Indeed, experimental studies have revealed that the occurrence of the MI transition and CMR in $La_{0.7}Ca_{0.3}MnO_3$ results mainly from the combination of the DE interaction between Mn^{3+} and Mn^{4+} ions and a strong JT effect [3,11]. This system has been found to undergo a discontinuous FOMT at the Curie temperature (T_C) [12,13], and the nature of FOMT is associated with a strong electron-phonon coupling and/or an intrinsic inhomogeniety in the material

* Corresponding author. Tel.: +1 813 974 47 14.
E-mail addresses: mphan@cas.usf.edu (M.H. Phan), sharihar@cas.usf.edu (H. Srikanth).

0925-8388/$ – see front matter © 2010 Elsevier B.V. All rights reserved.
doi:10.1016/j.jallcom.2010.07.223

that gives rise to competing coexisting ground states [14,15]. Meanwhile, the $La_{0.7}Sr_{0.3}MnO_3$ system (which is free from JT lattice distortions) has been found to undergo a continuous SOMT and exhibit a canonical magnetoresistance (MR) behavior [3,16]. From a crystal structure standpoint, we note that $La_{0.7}Ca_{0.3}MnO_3$ crystallizes in an orthorhombic (*Pbnm*) structure, whereas $La_{0.7}Sr_{0.3}MnO_3$ possesses a rhombohedral ($R\bar{3}c$) structure [17–19].

One way to stabilize intermediate phases bridging the two systems is co-substitution of both Sr and Ca in the lattice. The substitution of large Sr^{2+} ions for smaller Ca^{2+} ions in $La_{0.7}Ca_{0.3-x}Sr_xMnO_3$ ($0 \le x \le 0.3$) manganites leads to a structural change from the orthorhombic to rhombohedral structure which consequently results in the different properties of the materials [3,17,19]. Notably, Tomioka et al. [3] reported that with increasing Sr-doped content, the sharp MI transition and "colossal" MR behavior for $La_{0.7}Ca_{0.3}MnO_3$ ($x = 0$) were transformed to the metallic state and "canonical" MR behavior for $La_{0.7}Sr_{0.3}MnO_3$ ($x = 0.3$). However, the physical origin of the observed phenomena is still not fully understood. Particularly, the mechanism of a metal-like conductivity in the paramagnetic region in $La_{0.7}Ca_{0.3-x}Sr_xMnO_3$ compounds with $x > 0.1$ remains an open question [3]. In addition, it is unclear how the magnetic interactions are renormalized near the PM–FM transition range and what universality class governs the PM–FM transitions in these systems.

To address these important and as yet unresolved issues, we have conducted a comprehensive study of the ferromagnetic phase transitions and critical exponent trends near these transitions in $La_{0.7}Ca_{0.3-x}Sr_xMnO_3$ ($x = 0$, 0.05, 0.1, 0.2 and 0.25) single crystals. Based on the H/M vs. M^2 analyses and using Banerjee criterion, we demonstrate a transition from the discontinuous FOMT to the continuous SOMT at $x \sim 0.1$. The critical analyses, based on the magnetic data using the Kouvel–Fisher method, affirm that $x \sim 0.1$ is a tri-critical point that separates FOMT for $x < 0.1$ from SOMT for $x > 0.1$. Above the tri-critical point (e.g. $x = 0.2$), the system exhibits a SOMT with the critical exponents ($\beta = 0.36 \pm 0.01$, $\gamma = 1.22 \pm 0.01$) belonging to the Heisenberg universality class ($\beta = 0.365 \pm 0.003$, $\gamma = 1.336 \pm 0.004$) with short-range exchange interactions. This indicates that the magnetic interaction in these manganites is of short-range type. Our results and analyses reveal that while the DE mechanism and formation of ferromagnetic clusters can account for the canonical MR and metal-like conducting behavior in $La_{0.7}Ca_{0.3-x}Sr_xMnO_3$ with $x = 0.2$ and 0.25, other effects such as cooperative Jahn–Teller distortions and antiferromagnetic coupling are important additions for understanding the nature of the ferromagnetic transition, the MI transition and CMR in $La_{0.7}Ca_{0.3-x}Sr_xMnO_3$ with $x = 0$, 0.05 and 0.1. Our studies provide physical insights into the relationship between the ferromagnetism and conductivity in doped manganites.

2. Experimental

Single crystals of $La_{0.7}Ca_{0.3-x}Sr_xMnO_3$ ($x = 0$, 0.05, 0.1, 0.2, 0.25) were prepared by the floating-zone method using an infrared radiation convergence-type image furnace that consist of four mirrors and halogen lamps; details of the growth conditions can be found elsewhere [20]. The starting ceramic rods were obtained from the solid-state reaction of a stoichiometric mixture of La_2O_3, $CaCO_3$, $SrCO_3$ and $MnCO_3$. X-ray diffraction (XRD) data and electron-probe microanalysis confirmed the quality of the crystals. The XRD analyses indicated that the crystal structure is orthorhombic for $x = 0$, 0.05 and 0.1 compositions and is rhombohedral for $x = 0.2$ and 0.25 compositions. These results are fully consistent with those reported in previous works [17–19]. Magnetic measurements were performed using a commercial Physical Property Measurement System (PPMS) from Quantum Design in the temperature range of 2–350 K at applied fields up to 7 T. To extract the critical exponents of the samples accurately, the magnetic isotherms for all samples were measured in the range of 0–2 T and with a temperature interval of 1 K in the vicinity of their Curie temperatures (T_C).

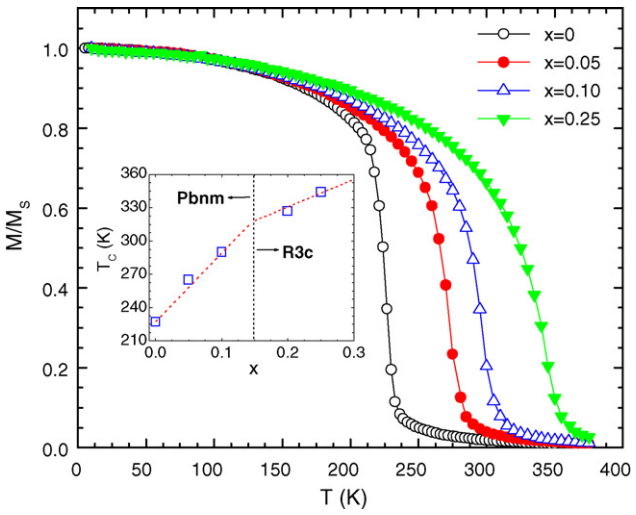

Fig. 1. Temperature dependence of magnetization taken at 5 kOe. Inset shows the dependence of the Curie temperature (T_C) on the S-doped content. The boundary line between the orthorhombic (*Pbnm*) and rhombohedral ($R\bar{3}c$) phases is taken at $x = 0.15$.

3. Results and discussion

Fig. 1 shows the temperature dependence of magnetization taken at an applied field of 5 kOe for $La_{0.7}Ca_{0.3-x}Sr_xMnO_3$ ($x = 0$, 0.05, 0.1 and 0.25) samples. It is observed in Fig. 1 that all the samples undergo a PM–FM transition and this transition broadens gradually with increasing Sr doping. The Curie temperatures (T_C) of the samples, which are defined by the minimum in dM/dT, are plotted as a function of Sr-doping, as shown in the inset of Fig. 1. In connection with the crystal structure of the samples, one can see clearly in the inset of Fig. 1 that with increasing Sr doping, the T_C increases at a rate faster in the orthorhombic phase ($x = 0$, 0.05 and 0.1) than in the rhombohedral phase ($x = 0.2$ and 0.25). The boundary line between these two crystalline phases is taken at $x = 0.15$, which corresponds to a tolerance factor $t = 0.92$ as determined from previous studies [3,19,21]. It has been noted in doped manganites that cooperative JT distortions are present in the orthorhombic phase but are not allowed due to the higher symmetry of the MnO_6 octahedra in the rhombohedral phase [22–24]. This thus leads to a general expectation in the present case that the JT effect is significant in $La_{0.7}Ca_{0.3-x}Sr_xMnO_3$ with $x = 0$, 0.05 and 0.1 but is negligible in $La_{0.7}Ca_{0.3-x}Sr_xMnO_3$ with $x = 0.2$ and 0.25. Since JT distortions decrease and the Mn–O–Mn bond angle increases (or W increases) with Sr doping, the DE interaction is strengthened and the metallic ferromagnetic state is stabilized in the samples with high Sr doping [3,17]. This clearly explains the increase of T_C with increasing Sr doping (see Fig. 1). This also explains a faster increasing rate of T_C with Sr addition in the orthorhombic phase than in the rhombohedral phase (see the inset of Fig. 1).

To determine the type of magnetic phase transition in $La_{0.7}Ca_{0.3-x}Sr_xMnO_3$ ($x = 0$, 0.05, 0.1, 0.2 and 0.25) samples, we have analyzed H/M vs. M^2 curves (which were converted from the isothermal M–H data) using Banerjee criterion [25] and the results of which are presented in Fig. 2. According to this criterion, the magnetic transition is of second order if all the H/M vs. M^2 curves have a positive slope [26]. On the other hand, if some of the H/M vs. M^2 curves show a negative slope at some point, the transition is of first order [26,27]. It can be observed in Fig. 2 that the H/M vs. M^2 curves of the $x = 0$ and 0.05 samples show a negative slope at $T > T_C$, indicating that the magnetic transition is of FOMT type for these samples. However, the H/M vs. M^2 curves of the $x = 0.1$, 0.2 and 0.25 samples have positive slopes, implying that these samples belong

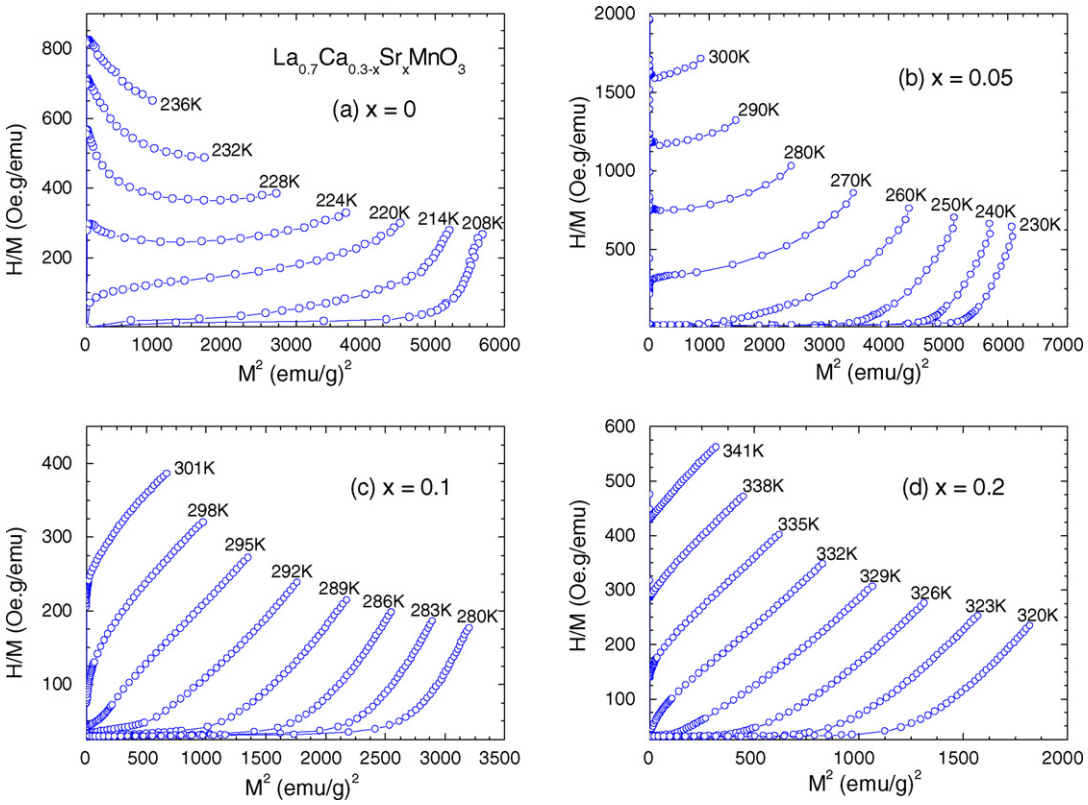

Fig. 2. The H/M vs. M^2 plots for representative temperatures around the T_C for the $La_{0.7}Ca_{0.3-x}Sr_xMnO_3$ ($x = 0$, 0.05, 0.1 and 0.2) samples.

to the class of SOMT materials. Nevertheless, a closer examination of the H/M vs. M^2 curves at low magnetic fields for $x = 0.1$ reveals that this sample is not a purely SOMT material and some degree of FOMT may be still present in the material. It has been noted that a precise determination of the type of magnetic transition using Banerjee criterion becomes difficult when the magnetic transition is a mixture of FOMT and SOMT [28]. Our study shows that the Sr doping in $La_{0.7}Ca_{0.3-x}Sr_xMnO_3$ ($x = 0$, 0.05, 0.1, 0.2 and 0.25) suppresses FOMT but favors SOMT and a FOMT to SOMT transition occurs at $x \sim 0.1$. A similar trend has been reported on polycrystalline $La_{2/3}(Ca_{1-x}Sr_x)_{1/3}MnO_3$ ($x = 0$, 0.05, 0.15 and 0.3) manganites [24,26].

Since the $La_{0.7}Ca_{0.3-x}Sr_xMnO_3$ ($x = 0.1$, 0.2 and 0.25) samples exhibit SOMT, we have used the Kouvel–Fisher (K–F) method [29] to determine precisely the critical exponents of these samples. This method consists of an iterative procedure which starts by constructing the Arrott–Noakes (A–N) plot (i.e. the plot of $M^{2.5}$ vs. $(H/M)^{0.75}$). From it, the values for $M_0(T)$ are computed from the intercepts of various isothermal magnetization vs. field curves on the ordinate of the plot (for temperatures below T_C). The intercept on the abscissa (for temperatures above T_C), allows calculating $\chi_0(T)$. Once the $M_0(T)$ and $\chi_0(T)$ curves have been constructed, two additional parameter data sets, $X(T)$ and $Y(T)$, may be determined:

$$X(T) = \chi_0^{-1}\left(\frac{d\chi_0^{-1}}{dT}\right)^{-1} = \frac{T - T_C}{\gamma} \quad (1)$$

$$Y(T) = M_0\left(\frac{dM_0}{dT}\right)^{-1} = \frac{T - T_C}{\beta} \quad (2)$$

In the critical region, both $X(T)$ and $Y(T)$ should be linear, with slopes which give the values of the critical exponents, and intercepts of the temperature axis which correspond to the Curie temperature. The values of the critical exponents are refined by using an iterative method: once Eqs. (1) and (2) produce the values of the critical exponents, a generalized Arrott–Noakes plot ($M^{1/\beta}$ vs. $(H/M)^{1/\gamma}$) is constructed and used to calculate new $M_0(T)$ and $\chi_0(T)$ curves, which are subsequently input into Eqs. (1) and (2), resulting in newer values for β and γ. The procedure terminates when the desired convergence of the parameters is achieved. T_C is obtained as the intercept on the abscissa of both X and Y lines.

Fig. 3 shows the A–N plots of the $La_{0.7}Ca_{0.3-x}Sr_xMnO_3$ ($x = 0.1$, 0.2 and 0.25) samples with optimized critical exponents (β and γ) obtained from the K–F method. Fig. 4 shows the K–F plot for one representative sample ($x = 0.2$). The best fits yield the values of $T_C = 289$ K, $\beta = 0.26 \pm 0.01$ and $\gamma = 1.06 \pm 0.02$ for the $x = 0.1$ sample; $T_C = 326$ K, $\beta = 0.36 \pm 0.01$ and $\gamma = 1.22 \pm 0.01$ for the $x = 0.2$ sample; $T_C = 344$ K, $\beta = 0.42 \pm 0.02$ and $\gamma = 1.14 \pm 0.05$ for the $x = 0.25$ sample. Using the Widom scaling relationship [30], $\beta + \gamma = \beta\delta$, the critical exponent (δ) is determined to be 5.1 ± 0.2, 4.4 ± 0.2 and 3.7 ± 0.2 for $x = 0.1$, 0.2 and 0.25 compositions, respectively. This relationship has been tested by plotting $M(T = T_C)$ versus $H^{\beta/(\beta+\gamma)} = H^{1/\delta}$ and checking the linearity of the curve as shown in Fig. 5.

The reliability of the obtained exponents and Curie temperatures can also be ascertained by checking the scaling of the magnetization curves. Two different constructions have been used in this work, both based on the scaling equation of state. For magnetic systems, the scaling equation of state takes the form [31]

$$\frac{H}{M^\delta} = h\left(\frac{\varepsilon}{M^{1/\beta}}\right), \quad (3)$$

where $\varepsilon = (T - T_C)/T_C$ is the reduced temperature, T_C is the Curie temperature, $h(x)$ is a scaling function and β and δ are critical exponents which characterize the magnetization behavior along coexistence ($H = 0$, $\varepsilon < 0$) and the critical isotherm ($\varepsilon = 0$), respectively. Eq. (3) may be formally inverted as:

$$\frac{M}{|\varepsilon|^\beta} = m_\pm\left(\frac{H}{|\varepsilon|^\Delta}\right), \quad (4)$$

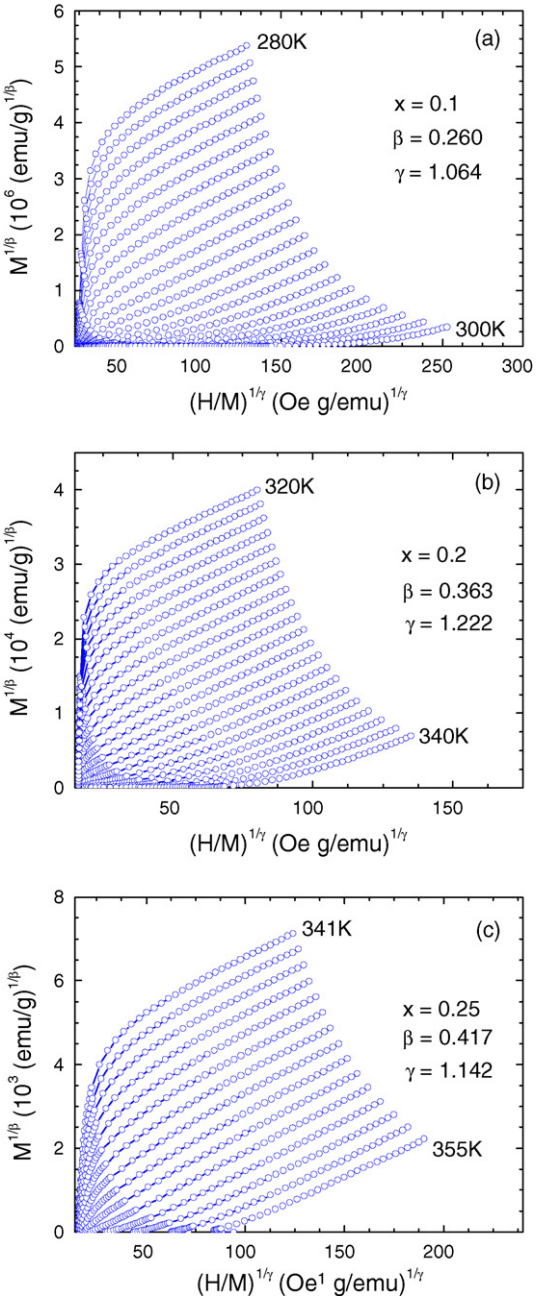

Fig. 3. Modified Arrott plot isotherms with 1 K temperature interval for the $La_{0.7}Ca_{0.3-x}Sr_xMnO_3$ ($x = 0.1$, 0.2 and 0.25) samples.

where $\Delta = \beta\delta$ is the gap exponent, and the plus (minus) sign corresponds to $\varepsilon > 0$ ($\varepsilon < 0$), respectively. Therefore, according to Eq. (3), if the appropriate values for the critical exponents and for the Curie temperature are used, the plot of $M/H^{1/\delta}$ versus $\varepsilon/H^{1/\Delta}$ should correspond to a universal curve onto which all experimental data points collapse. Alternatively, Eq. (4) indicates that $M/|\varepsilon|^{\beta}$ versus $H/|\varepsilon|^{\Delta}$ should result in two universal curves, one for $\varepsilon > 0$ and the other for $\varepsilon < 0$. For a more convenient visualization of the results, this plot is usually represented in logarithmic scale. However, this second representation tends to cover the small deviations of the experimental data with respect to the universal curves caused by an inappropriate choice of the parameters. Using the values of β, γ and T_C obtained from the K–F method, the scaled data are plotted in Fig. 6 for the $x = 0.1$ and 0.2 samples, respectively. In the case of scaling using Eq. (4), it can be observed that all the experimental points

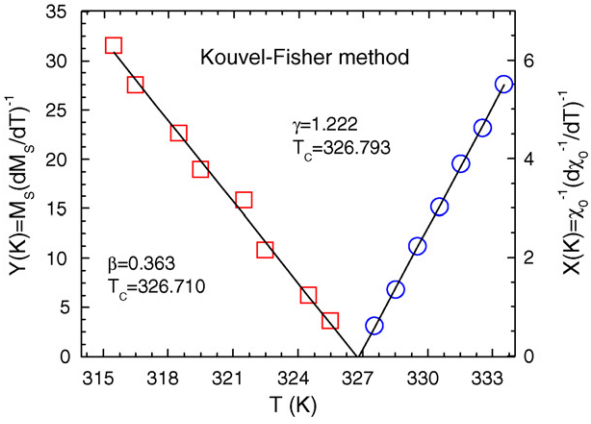

Fig. 4. Temperature dependence of spontaneous M_s (square) and inverse initial susceptibility χ_0^{-1} (circles) for the $x = 0.2$ sample; solid lines are fitting curves to Eqs. (1) and (2), respectively.

fall on two curves, one for $T < T_C$ and the other for $T > T_C$. This clearly indicates that the obtained values of β, γ and T_C for these samples are reliable and in agreement with the scaling hypothesis. A less perfect overlap of the data points has been observed for the $x = 0.1$ sample in comparison with the $x = 0.2$ sample (see Fig. 6a and b). This agrees with our previous observation (Fig. 2c) and argument that this sample is not a purely SOMT material and some degree of FOMT is still present in it.

To put our obtained results in the context of previous works, we summarize in Table 1 the values of the critical exponents of $La_{0.7}Ca_{0.3-x}Sr_xMnO_3$ ($x = 0.1$, 0.2 and 0.25) samples, of different theoretical models [32,33] and of other manganites in the literature [34–60]. It has been argued that in homogeneously magnetic systems the universality class of the magnetic phase transition should depend on the range of the exchange interaction, $J(r)$ [61]. If $J(r)$ decays with distance (r) at a rate faster than r^{-5} then the Heisenberg exponents ($\beta = 0.365 \pm 0.003$, $\gamma = 1.336 \pm 0.004$) are valid for a 3D isotropic ferromagnet [32]. However, if $J(r)$ decays at a rate slower than $r^{-4.5}$ then the mean-field exponents ($\beta = 0.5$, $\gamma = 1$) are valid. According to the DE theory, the effective ferromagnetic interaction is driven by the kinetics of the electrons which favor extended states. Therefore, one could expect the critical exponents in the DE model to be described within the framework of the mean-field theory [35,62]. However, computational studies have demonstrated that the critical exponents in the DE model are con-

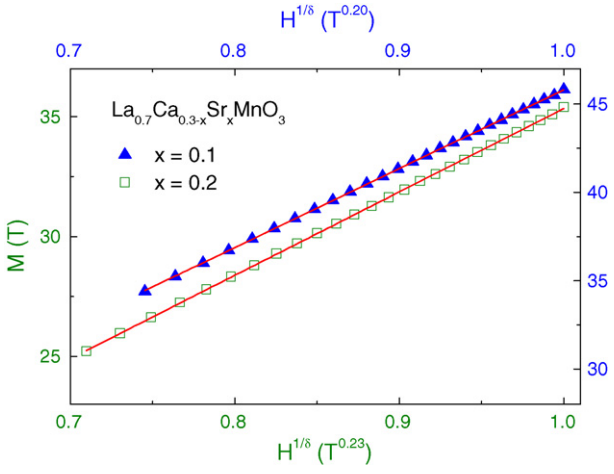

Fig. 5. The linearity of the $M(T = T_C)$ versus $H^{\beta/(\beta+\gamma)} = H^{1/\delta}$ curves validates the value of δ calculated using the Widom relationship with the experimental data.

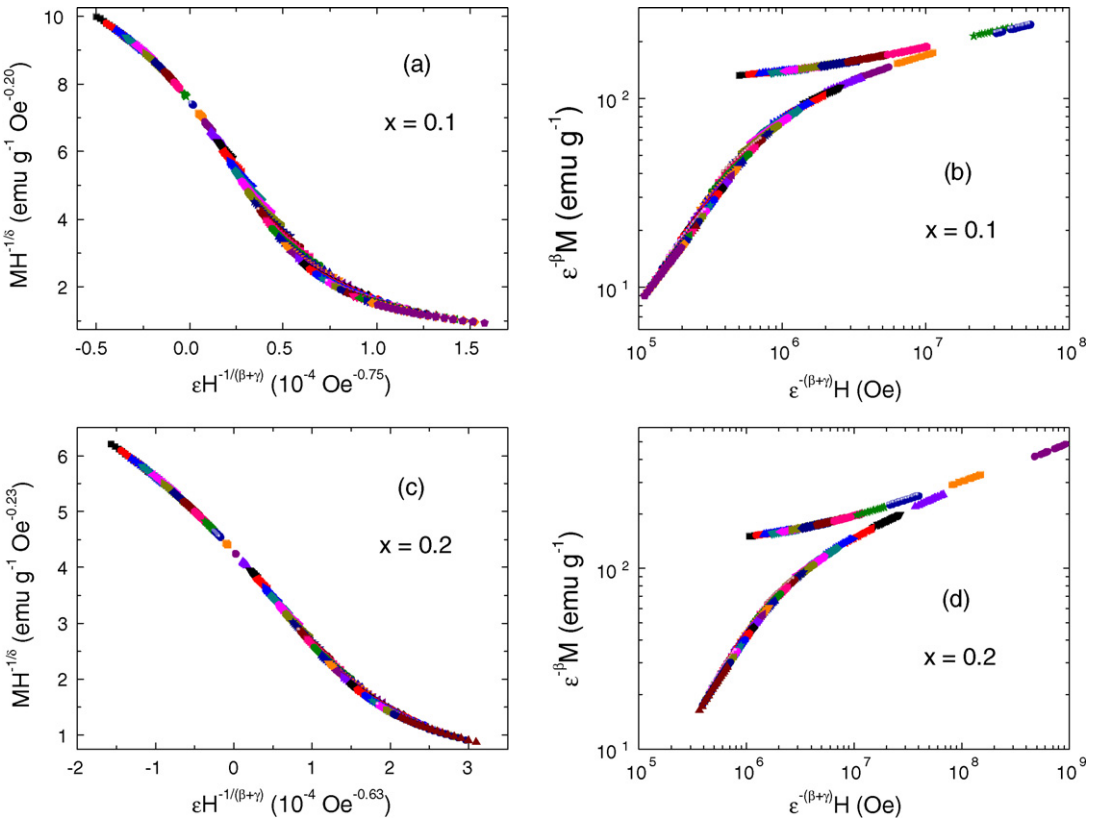

Fig. 6. Normalized isotherms of $La_{0.7}Ca_{0.3-x}Sr_xMnO_3$ ($x = 0.1$ and 0.2) samples below and above Curie temperature (T_C) using the values of β and γ determined using from the K–F method.

Table 1
Comparison of the values of the critical exponents of $La_{0.7}Ca_{0.3-x}Sr_xMnO_3$ ($x = 0.1$, 0.2 and 0.25) single crystals with those of theoretical models and of other manganites in the literature. Bulk magnetization technique was used for studying the critical properties of all samples compared. SC: single crystal; PC: polycrystal; TF: thin film.

Material	Structure	T_C (K)	β	γ	δ	Reference
$La_{0.7}Ca_{0.2}Sr_{0.1}MnO_3$ (SC)	Orthorhombic	289	0.26 ± 0.01	1.06 ± 0.02	5.1 ± 0.2	This work
$La_{0.7}Ca_{0.1}Sr_{0.2}MnO_3$ (SC)	Rhombohedral	326	0.36 ± 0.01	1.22 ± 0.01	4.4 ± 0.2	This work
$La_{0.7}Ca_{0.05}Sr_{0.25}MnO_3$ (SC)	Rhombohedral	344	0.42 ± 0.02	1.14 ± 0.05	3.7 ± 0.2	This work
$La_{0.7}Sr_{0.3}MnO_3$ (SC)	Rhombohedral	360	0.45 ± 0.02	1.08 ± 0.04	3.4 ± 0.3	[38]
Mean-field model			0.5	1.0	3.0	[32]
3D Heisenberg model			0.365 ± 0.003	1.336 ± 0.004	4.80 ± 0.04	[32]
3D Ising model			0.325 ± 0.002	1.241 ± 0.002	4.82 ± 0.02	[32]
Tricritical mean-field model			0.25	1	5	[33]
$La_{0.7}Ca_{0.3}MnO_3$ (SC)	Orthorhombic	222	0.14 ± 0.02	0.81 ± 0.03	1.22 ± 0.04	[39]
$La_{0.6}Ca_{0.4}MnO_3$ (PC)	Orthorhombic	265	0.25 ± 0.03	1.03 ± 0.05	5.0 ± 0.8	[33]
$La_{0.67}Ca_{0.33}Mn_{0.9}Ga_{0.1}O_3$ (PC)	Orthorhombic	116	0.387 ± 0.006	1.36 ± 0.002	4.6 ± 0.03	[46]
$La_{0.67}Ca_{0.33}MnO_3$ (TF)	Orthorhombic	261	0.368 ± 0.003	1.384 ± 0.001	4.76 ± 0.32	[41]
$La_{0.875}Sr_{0.125}MnO_3$ (SC)	Rhombohedral	186	0.37 ± 0.02	1.38 ± 0.03	4.72 ± 0.04	[44]
$La_{0.75}Sr_{0.25}MnO_3$ (SC)	Rhombohedral	346	0.40 ± 0.02	1.27 ± 0.06	4.12 ± 0.33	[40]
$La_{0.7}Sr_{0.3}MnO_3$ (SC)	Rhombohedral	354	0.37 ± 0.04	1.22 ± 0.03	4.25 ± 0.2	[34]
$La_{0.67}Ba_{0.33}MnO_3$ (PC)	Rhombohedral	306	0.356 ± 0.004	1.120 ± 0.003	4.15 ± 0.05	[36]
$La_{0.9}Pb_{0.1}MnO_3$ (PC)	Pseudo-rhombohedral	162	0.498	1.456	3.92	[50]
$Nd_{0.85}Pb_{0.15}MnO_3$ (SC)	Tetragonal	109	0.372 ± 0.004	1.347 ± 0.001	4.67 ± 0.03	[49]
$Nd_{0.7}Pb_{0.3}MnO_3$ (SC)	Tetragonal	148	0.361 ± 0.013	1.325 ± 0.001	4.62 ± 0.04	[49]
$Nd_{0.6}Pb_{0.4}MnO_3$ (SC)	Tetragonal	156	0.374 ± 0.006	1.329 ± 0.003	4.54 ± 0.10	[43]
$Pr_{0.77}Pb_{0.23}MnO_3$ (SC)	Pseudocubic	167	0.344 ± 0.001	1.352 ± 0.006	4.69 ± 0.02	[55]
$Pr_{0.7}Pb_{0.3}MnO_3$ (SC)	Pseudocubic	197	0.404 ± 0.001	1.357 ± 0.006	4.37 ± 0.09	[55]
$LaMn_{0.95}Ti_{0.05}MnO_3$ (PC)	Rhombohedral	172	0.378 ± 0.007	1.29 ± 0.02	4.19 ± 0.03	[54]
$LaMn_{0.9}Ti_{0.1}MnO_3$ (PC)	Rhombohedral	145	0.375 ± 0.005	1.25 ± 0.02	4.11 ± 0.04	[54]
$LaMn_{0.85}Ti_{0.15}MnO_3$ (PC)	Rhombohedral	121	0.376 ± 0.003	1.24 ± 0.01	4.16 ± 0.03	[54]
$LaMn_{0.8}Ti_{0.2}MnO_3$ (PC)	Rhombohedral	95	0.359 ± 0.004	1.28 ± 0.01	4.21 ± 0.05	[54]
$La_{0.9}Te_{0.1}MnO_3$ (PC)	Orthorhombic	239	0.201 ± 0.003	1.27 ± 0.04	7.14 ± 0.04	[53]
$Pr_{0.5}Sr_{0.5}MnO_3$ (PC)	Orthorhombic	261	0.443 ± 0.002	1.339 ± 0.006	4 ± 0.003	[57]
$Nd_{0.5}Sr_{0.5}MnO_3$ (PC)	Orthorhombic	239	0.5 ± 0.001	1.02 ± 0.02	4.02 ± 0.05	[51]
$LaMnO_{3.14}$ (PC)	Rhombohedral	141	0.415	1.470	4.542	[37]

sistent with those expected for the 3D Heisenberg model [63]. It has also been theoretically shown that PM–FM transitions may become discontinuous, depending on doping level and competition with superexchange AFM interactions [64].

The values of the critical exponents of $La_{0.7}Ca_{0.3-x}Sr_xMnO_3$ ($x = 0.1$, 0.2 and 0.25) samples are in agreement with those predicted by the latter models [63,64]. It is clear in Table 1 that the critical exponents of the $x = 0.1$ sample ($\beta = 0.26 \pm 0.01$, $\gamma = 1.06 \pm 0.02$) match well with those derived from the tricritical mean-field model ($\beta = 0.25$, $\gamma = 1$). The existence of this tricritical point ($x \sim 0.1$) clearly sets a boundary between FOMT ($x < 0.1$) and SOMT ($x > 0.1$) with the ferromagnetic range ($0 \leq x \leq 0.25$). A similar case has also been reported on $La_{1-x}Ca_xMnO_3$ ($0.2 \leq x \leq 0.5$) polycrystalline manganites, where the tricritical point is found at $x \sim 0.4$ [33]. To further confirm that the PM–FM transition becomes a conventional SOMT above the tricritical point, the critical exponents of the samples with $x > 0.1$ are expected to match those predicted for the 3D Heisenberg model [53]. As one can see clearly in Table 1, the values of the critical exponents of the $x = 0.2$ sample ($\beta = 0.36 \pm 0.01$, $\gamma = 1.22 \pm 0.01$) are close to those expected for the 3D Heisenberg model ($\beta = 0.365 \pm 0.003$, $\gamma = 1.336 \pm 0.004$). For the $x = 0.25$ sample, the value of $\beta = 0.42 \pm 0.02$ is relatively larger than that expected for the 3D Heisenberg model ($\beta = 0.365 \pm 0.003$) but is consistent with that of $La_{0.7}Sr_{0.3}MnO_3$ ($\beta = 0.45 \pm 0.02$) reported previously by Ziese [38] and Taran et al. [47] using the A–N method and by Lofland et al. [16] using microwave absorption methods. The critical exponent of the $x = 0.25$ sample ($\gamma = 1.14 \pm 0.05$) is smaller than that of the $x = 0.2$ sample ($\gamma = 1.22 \pm 0.01$). A gradual decrease of γ with Sr addition is clearly seen in Table 1 for $La_{0.7}Ca_{0.3-x}Sr_xMnO_3$ ($x = 0.2$ and 0.25) reported by us and for $La_{0.7}Sr_{0.3}MnO_3$ ($x = 0.3$) reported by Ziese [38]. It has been argued that for a true SOMT the critical exponents are independent of the microscopic details of a system due to the divergence of correlation length and correlation time close to a transition point and hence their values are almost the same for a transition that may occur in different physical systems [31]. This hypothesis has been experimentally validated for the case of $Nd_{1-x}Pb_xMnO_3$ ($x = 0.15$, 0.3 and 0.4) [43,49] and $LaMn_{1-x}Ti_xO_3$ ($x = 0.05$, 0.1 and 0.15) [54], where the critical exponents (both β and γ) are almost Pb- (or Ti) doping independent and are consistent with those expected for the 3D Heisenberg model. However, one must note secondary effects on the PM–FM transition (hence on the critical exponents) of a system due to magnetic anisotropies or dipolar long-range couplings of ferromagnetic clusters [42,48,50,65]. It has been pointed out that a Mn-ion triplets containing a Mn^{3+}–Mn^{4+}–Mn^{3+} cluster has significant binding energy of about half the binding energy of the bulk [66]. The large spin moments of these ferromagnetic clusters are expected to enhance the dipole–dipole interaction in the case of the 3D Heisenberg model thus resulting in larger values of the critical exponents than those predicted by this model [47,66]. Recently, magnetization and electron paramagnetic resonance (EPR) studies have revealed that ferromagnetic clusters persisting even in the paramagnetic region have significant influence on the magnetic order parameters (i.e. the critical exponents) in doped manganites, such as $La_{0.9}Pb_{0.1}MnO_3$ ($\beta = 0.498$, $\gamma = 1.456$) [50] and $Pr_{0.5}Sr_{0.5}MnO_3$ ($\beta = 0.443 \pm 0.002$, $\gamma = 1.339 \pm 0.006$) [57,67].

In the case of $La_{0.7}Ca_{0.3-x}Sr_xMnO_3$ ($x = 0.1$, 0.2 and 0.25) samples, the $x = 0.1$ composition is on the crossover region of FOMT → SOMT. This composition has also been noted to be on the crossover region of a MI transition (for $x < 0.1$ compositions the MI transition is well defined, but this transition is largely suppressed and instead a metal-like conducting behavior is observed in the paramagnetic region for $x > 0.1$ compositions) [3]. This coincidence clearly demonstrates a coherent correlation between the magnetism and conductivity in the doped manganites. Furthermore, we note the nonlinearity of the modified Arrott plots (Fig. 3), signalling the nature of ferromagnetic clusters in the $La_{0.7}Ca_{0.3-x}Sr_xMnO_3$ samples [43,49,55]. The formation of ferromagnetic clusters in these samples has been evidenced from EPR spectra [68]. Therefore, it can be proposed that it is the formation of ferromagnetic clusters that leads to a percolation mechanism for conduction and metallic behaviors observed at $T > T_C$ in the paramagnetic region for the $x = 0.2$ and 0.25 samples [55,69]. A recent study has shown that the PM–FM transition of a $(Sm_{0.7}Nd_{0.3})_{0.52}Sr_{0.48}MnO_3$ manganite transforms from a FOMT to a SOMT when subjected to an external pressure [58]. The critical exponents of this sample ($\beta = 0.358$, $\gamma = 1.297$) under external pressure are close to those expected for the 3D Heisenberg model ($\beta = 0.365$, $\gamma = 1.336$). It has been argued that the presence of external pressure at a certain level can suppress the polaronic state, increase the bandwidth (W) of the system, and as a result the FOMT converts to SOMT [58]. In the case of $La_{0.7}Ca_{0.3-x}Sr_xMnO_3$ ($x = 0$, 0.05, 0.1, 0.2 and 0.25) manganites, we argue that the substitution of large Sr^{2+} ions ($\langle r_A \rangle \sim 1.31$ Å) for smaller Ca^{2+} ions ($\langle r_A \rangle \sim 1.18$ Å) introduces chemical (internal) pressure without affecting the valency of the Mn ions (the ratio of Mn^{3+}/Mn^{4+} is unchanged or no change of electronic density) [18,19]. It has been shown that the chemical pressure modifies local structural parameters such as the Mn–O bond distance and Mn–O–Mn bond angle, which directly influence the case of electron hopping between Mn ions (i.e. the electronic bandwidth – W) [1,3,18,19]. Therefore, the change of internal pressure with Sr addition is expected to increase W which consequently increases the T_C and converts the FOMT into SOMT at a threshold pressure (which corresponds to a Sr-doping level, $x = 0.1$). Above the critical point ($x > 0.1$), the system shows a SOMT with the critical exponents belonging to the Heisenberg universality class. The change in nature of the PM–FM transition with chemical (internal) pressure (Sr doping) clearly points to a strong coupling between the magnetic order parameter and lattice strain in these doped manganites [58].

Furthermore, the theory predicts that the PM–FM transition of $La_{1-x}M_xMnO_3$ (M = Ca, Sr) becomes continuous or discontinuous, depending upon the change in the relative strength of the DE interaction (i.e. the FM interaction) and AFM coupling [64]. In the present study, we note that the ground state of $La_{0.7}Ca_{0.3}MnO_3$ ($x = 0$) is ferromagnetic, but the AFM phase is also present and competing with the FM phase [14,15]. The substitution of Sr for Ca in $La_{0.7}Ca_{0.3-x}Sr_xMnO_3$ ($x = 0$, 0.05, 0.1, 0.2 and 0.25) suppresses the AFM phase while it enhances the FM phase. As a result, the PM–FM transition changes from discontinuous to continuous at $x \sim 0.1$. In addition, we recall that strong JT lattice distortions are possible in the $x = 0$, 0.05 and 0.1 samples that crystallize in an orthorhombic structure, whereas this effect is negligible in the $x = 0.2$ and 0.25 samples possessing a rhombohedral structure. These important observations, coupled with the magnetic, magnetotransport and critical exponent analyses, clearly suggest that in addition to the DE interaction, cooperative JT effects and AFM coupling are important ingredients for assessing the nature of the ferromagnetic transition and the MI transition including CMR in $La_{0.7}Ca_{0.3-x}Sr_xMnO_3$ ($x = 0$, 0.05 and 0.1) manganites. While the DE model is sufficient to explain the canonical MR behavior in $La_{0.7}Ca_{0.3-x}Sr_xMnO_3$ ($x = 0.2$ and 0.25) samples where AFM interactions are weak and JT lattice distortions are negligible, the formation of ferromagnetic clusters likely leads to a percolation mechanism for the conduction and metallic behavior observed in the paramagnetic region for these samples.

4. Conclusions

The ferromagnetic phase transitions and critical behavior of $La_{0.7}Ca_{0.3-x}Sr_xMnO_3$ ($x = 0$, 0.05, 0.1, 0.2 and 0.25) single crystals

have been studied systematically. Using Banerjee criterion and Kouvel–Fisher method, we show that $x \sim 0.1$ is a tricritical point that separates FOMT for $x < 0.1$ from SOMT for $x > 0.1$. Above the tricritical point, the system exhibits a SOMT with the critical exponents belonging to the Heisenberg universality class with short-range exchange interactions. This indicates that the magnetic interaction in these systems is of short-range type. We show that while the DE mechanism and formation of ferromagnetic clusters can account for the canonical MR and metal-like conducting behavior in $La_{0.7}Ca_{0.3-x}Sr_xMnO_3$ with $x = 0.2$ and 0.25, other effects such as cooperative Jahn–Teller distortions and antiferromagnetic coupling are important additions for understanding the relationship between the PM–FM transition and MI transition, including CMR in $La_{0.7}Ca_{0.3-x}Sr_xMnO_3$ with $x = 0$, 0.05 and 0.1. The change of the PM–FM transition with chemical (internal) pressure introduced by substitution of larger Sr ions for smaller Ca ions points to the strong coupling between the magnetic order and structural parameters in these doped manganites.

Acknowledgements

This work is supported by the Department of Army through grant number W911NF-08-1-0276. HS and MHP also thank the Department of Energy BES for support through grant number DE-FG02-07ER46438. VF acknowledges the Spanish Ministry of Science and Innovation and EU FEDER (Projects MAT 2007-65227 and MAT 2010-20537), and the PAI of the Regional Government of Andalucía.

References

[1] Y. Tokura, Y. Tomioka, Magn. Magn. Mater. 200 (1999) 1–23.
[2] P.G. Radaelli, D.E. Cox, M. Marezio, S.-W. Cheong, P.E. Schifer, A.P. Ramirez, Phys. Rev. Lett. 75 (1995) 4488–4491.
[3] Y. Tomioka, A. Asamitsu, Y. Tokura, Phys. Rev. B 63 (2000) 024421.
[4] H.Y. Hwang, S.W. Cheong, P.G. Radaelli, M. Marezio, B. Batlogg, Phys. Rev. Lett. 75 (1995) 914–917.
[5] E. Dagotto, New J. Phys. 7 (2005) 67.
[6] B. By Vijay, C.N. Shenoy, Rao, Phil. Trans. R. Soc. A 366 (2008) 63–82.
[7] J. Tao, D. Niebieskikwiat, M. Varela1, W. Luo, M.A. Schofield, Y. Zhu, M.B. Salamon, J.M. Zuo, S.T. Pantelides, S.J. Pennycook, Phys. Rev. Lett. 103 (2009) 097202.
[8] C. Zener, Phys. Rev. 82 (1951) 403–405.
[9] P.W. Anderson, H. Hasegawa, Phys. Rev. 100 (1955) 675–681.
[10] Y. Motome, N. Furukawa, Phys. Rev. B 71 (2005) 014446.
[11] P. Dai, J. Zhang, H.A. Mook, S.-H. Liou, P.A. Dowben, E.W. Plummer, Phys. Rev. B 54 (1996) R3694.
[12] C.S. Hong, W.S. Kim, N.H. Hur, Phys. Rev. B 63 (2001) 092504.
[13] A.N. Ulyanov, J.S. Kim, Y.M. Kang, D.G. Yoo, S.I. Yoo, J. Appl. Phys. 104 (2008) 113916.
[14] A.S. Alexandrov, A.M. Bratkovsky, Phys. Rev. Lett. 82 (1999) 141–144.
[15] J.A. Verges, V. Martin-Mayor, L. Brey, Phys. Rev. Lett. 88 (2002) 136401.
[16] S.E. Lofland, V. Ray, P.H. Kim, S.M. Bhagat, M.A. Manheimer, S.D. Tyagi, Phys. Rev. B 55 (1997) 2749–2751.
[17] P.G. Radaelli, M. Marezio, H.Y. Hwang, S.-W. Cheong, B. Batlogg, Phys. Rev. B 54 (1996) 8992–8995.
[18] A.N. Ulyanov, G.V. Gusakov, V.A. Borodin, N.Yu. Starostyuk, A.B. Mukhin, Sol. Stat. Commun. 118 (2001) 103–105.
[19] A.N. Ulyanov, I.S. Maksimov, E.B. Nyeanchi, Yu.V. Medvedev, S.C. Yu, N.Yu. Starostyuk, B. Sundqvist, J. Appl. Phys. 91 (2002) 7739.
[20] C.S. Hong, W.S. Kim, E.O. Chi, K.W. Lee, N.H. Hur, Chem. Mater. 12 (2000) 3509.
[21] P.G. Radaelli, G. Iannone, M. Marezio, H.Y. Hwang, S.-W. Cheong, J.D. Jorgensen, D.N. Argiriou, Phys. Rev. B 56 (1997) 8265–8276.
[22] J.B. Goodenough, J. Appl. Phys. 81 (1997) 5330.
[23] C.H. Booth, F. Bridges, G.H. Kwei, J.M. Lawrence, A.L. Cornelius, J.J. Neumeier, Phys. Rev. Lett. 80 (1998) 853–856.
[24] J. Mira, J. Rivas, L.E. Hueso, F. Rivadulla, M.A. Lopez Quintela, J. Appl. Phys. 91 (2002) 8903.
[25] S.K. Banerjee, Phys. Lett. 12 (1964) 16.
[26] J. Mira, J. Rivas, F. Rivadulla, C. Vazquez, M.A. Lopez-Quintela, Phys. Rev. B 60 (1999) 2998–3001.
[27] M.H. Phan, S.C. Yu, N.H. Hur, Y.H. Jeong, J. Appl. Phys. 96 (2004) 1154.
[28] V. Franco, A. Conde, V. Provenzano, R.D. Shull, J. Magn. Magn. Mater. 322 (2010) 218–223.
[29] J.S. Kouvel, M.E. Fisher, Phys. Rev. 136 (1964) A1626.
[30] B. Widom, J. Chem. Phys. 43 (1965) 3898.
[31] H. Eugene Stanley, Introduction to Phase Transitions and Critical Phenomena, Oxford University Press, New York, 1971.
[32] M. Seeger, S.N. Kaul, H. Kronmuller, R. Reisser, Phys. Rev. B 51 (1995) 12585–12594.
[33] D. Kim, B. Revaz, B.L. Zink, F. Hellman, J.J. Rhyne, J.E. Mitchell, Phys. Rev. Lett. 89 (2002) 227202.
[34] K. Ghosh, C.J. Lobb, R.L. Greene, S.G. Karabashev, D.A. Shulyatev, A.A. Arsenov, Y. Mukovskii, Phys. Rev. Lett. 81 (1998) 4740–4743.
[35] Ch.V. Mohan, M. Seeger, H. Kronmuller, P. Murugaraj, J. Maier, J. Magn. Magn. Mater. 183 (1998) 348–355.
[36] N. Mautis, I. Panagiotopoulos, M. Pissas, D. Niarchos, Phys. Rev. B 59 (1999) 1129–1133.
[37] R.S. Freitas, C. Haetinger, P. Pureur, J.A. Alonso, L. Ghivelder, J. Magn. Magn. Mater. 226–230 (2001) 569–571.
[38] M. Ziese, J. Phys.: Condens. Matter 13 (2001) 2919.
[39] H.S. Shin, J.E. Lee, Y.S. Nam, H.L. Ju, C.W. Park, Sol. Stat. Commun. 118 (2001) 377.
[40] D. Kim, B.L. Zink, F. Hellman, J.M.D. Coey, Phys. Rev. B 65 (2002) 214424.
[41] A. Berger, G. Camopillo, P. Vivas, J.E. Pearson, S.D. Bader, E. Baca, P. Prieto, J. Appl. Phys. 91 (2002) 8393.
[42] H. Huhtinen, R. Laiho, E. Lahderanta, J. Salminen, K.G. Lisunov, V.S. Zakhvalinskii, J. Appl. Phys. 91 (2002) 7944.
[43] M. Sahana, U.K. Rossler, N. Ghosh, S. Elizabeth, H.L. Bhat, K. Dorr, D. Eckert, M. Wolf, K.-H. Muller, Phys. Rev. B 68 (2003) 144408.
[44] S. Nair, A. Banerjee, A.V. Narlikar, D. Prabhakaran, A.T. Boothroyd, Phys. Rev. B 68 (2003) 132404.
[45] A. Oleaga, A. Salazar, D. Prabhakaran, A.T. Boothroyd, J. Appl. Phys. 95 (2004) 7366.
[46] S. Roler, U.K. Roler, K. Nenkov, D. Eckert, S.M. Yusuf, K. Korr, K.-H. Muller, Phys. Rev. B 70 (2004) 104417.
[47] S. Taran, B.K. Chaudhuri, S. Chatterjee, H.D. Yang, S. Neeleshwar, Y.Y. Chen, J. Appl. Phys. 98 (2005) 103903.
[48] M. Kar, A. Perumal, S. Ravi, Phys. Stat. Sol 243 (2006) 1908.
[49] N. Ghosh, S. Roler, U.K. Roler, K. Nenkov, S. Elizabeth, H.L. Bhat, K. Dorr, K.-H. Muller, J. Phys.: Condes. Matter 18 (2006) 557.
[50] T.L. Phan, S.G. Min, S.C. Yu, S.K. Oh, J. Magn. Magn. Mater 304 (2006) e778.
[51] R. Venkatesh, R. Nirmala, G. Rangarajan, S.K. Malik, V. Sankaranarayanan, J. Appl. Phys. 99 (08) (2006) Q311.
[52] R. Venkatesh, M. Pattabiraman, K. Sethupathi, G. Rangarajan, S. Narayana, V. Sankaranarayanan, J. Appl. Phys. 101 (09) (2007) C506.
[53] J. Yang, Y.P. Lee, Y. Li, Phys. Rev. B 76 (2007) 054442.
[54] J. Yang, Y.P. Lee, Appl. Phys. Lett. 91 (2007) 142512.
[55] B. Padmanabhan, H.L. Bhat, S. Elizabeth, S. Robler, U.K. Robler, K. Dorr, K.H. Muller, Phys. Rev. B 75 (2007) 024419.
[56] A.G. Gamzatov, K. Sh Khizriev, A.B. Batdalov, Sh.B. Abdulvagidov, A.M. Aliev, Low Temp. Phys. 35 (2009) 214.
[57] A.K. Pramanik, A. Banerjee, Phys. Rev. B 79 (2009) 214426.
[58] P. Sarkar, S. Arumugam, P. Mandal, A. Murugeswari, R. Thiyagarajan, S. Esaki Muthu, D. Mohan Radheep, C. Ganguli, K. Matsubayshi, Y. Uwatoko, Phys. Rev. Lett. 103 (2009) 057205.
[59] N.V. Khiem, P.T. Phong, L.V. Bau, D.N.H. Nam, L.V. Hong, N.X. Phuc, J. Magn. Magn. Mater. 321 (2009) 2027.
[60] X. Zhu, Y. Sun, X. Luo, H. Lei, B. Wang, W. Song, Z. Yang, J. Dai, D. Shi, S. Dou, J. Magn. Magn. Mater. 322 (2010) 242.
[61] M.E. Fisher, S.K. Ma, B.G. Nickel, Phys. Rev. Lett. 29 (1972) 917.
[62] K. Kubo, N. Ohata, J. Phys. Soc. Jpn 33 (1972) 21.
[63] Y. Motome, N. Furukawa, J. Phys. Soc. Jpn 68 (1999) 3853.
[64] J.L. Alonso, L.A. Fernández, F. Guinea, V. Laliena, V. Martín-Mayor, Phys. Rev. B 63 (2001) 064416.
[65] M. Seeger, S.N. Kaul, H. Kronmüller, R. Reisser, Phys. Rev. B 51 (1995) 12585.
[66] G.A. Gehring, D.J. Coombes, J. Magn. Magn. Mater. 873 (1998) 177.
[67] S. Cao, B. Kang, J. Zhang, S. Yuan, Appl. Phys. Lett. 88 (2006) 172503.
[68] M. H. Phan et al. unpublished data.
[69] R.W. Li, X. Zhou, B.G. Shen, B. Hillebrands, Phys. Rev. B 71 (2005) 092407.